 

PACS numbers: 42.60.Fc; 42.70.Nq; 42.65.Re
DOI: 10.1070/QE2009v039n10ABEH014047

# Transient light absorption induced in glass by femtosecond laser pulses

I.V. Blonskyi, V.N. Kadan, O.I. Shpotyuk, I.A. Pavlov, N.N. Kryuchkov

*Abstract*. **The dynamics of the transient light absorption induced in K8 optical glass by filamented femtosecond laser pulses have been studied using time-resolved transmitted-light microscopy at wavelengths from 450 to 700 nm. The transient absorption measured as a function of probe beam wavelength is compared to that predicted by the Drude plasma model. We conclude that, just 450 fs after a pump pulse, the transient absorption is dominated by transient electronic states, presumably, self-trapped excitons, with an excitation energy of 2.6 – 2.7 eV. These states are filled with free-carriers from a long-lived plasma, which acts as a 'carrier reservoir'. The relaxation of transient absorption has two components. The slow component, with $\tau_1 \sim 17 - 17.5$ ps, is governed by the plasma thermalisation time, whereas the second, with $\tau_2 \gg 300$ ps, is determined by the plasma lifetime.**

***Keywords***: *femtosecond laser, plasma, induced absorption, optical glass, filament*.

## 1. Introduction

Systematic studies of high-power femtosecond laser pulse propagation in transparent media is central to the femtosecond optics of materials, a new, promising area of research. It is known [1, 2] that, in almost all transparent media, from gases to solids, femtosecond beams undergo filamentation and break up into separate components, whose diameter (several microns) remains constant over many Rayleigh lengths. Several models of beam filamentation have been proposed to date: moving foci [3], self-channelling [4], a dynamic model [5, 6], and X-waves [7] (see Ref. [2]). Filament dynamics in a variety of media were studied, e.g., by femtosecond time-resolved optical polarigraphy (FTOP) [8 – 14] and time-resolved transmitted-light microscopy (TTLM) [15 – 18]. Several studies addressed the kinetics of filament-induced transient light absorption (TLA) in glass targets [16 – 18]. The proposed mechanisms of TLA differ markedly. Generally, these mechanisms can be divided into two distinct groups: absorption of probe radiation by the nonequilibrium plasma generated in the filament core, according to the Drude model [18], and light absorption through transitions from the ground state to an excited level of transient electronic states (TESs) [16, 17] resulting from plasma relaxation. The term TESs is used to mean the formation and relaxation of self-trapped excitons, short-lived electronic excitations localised at traps, photo-induced short-lived structural defects etc. Analysis of the very limited information about TLA kinetics in an individual filament lends support to the two above approaches to TLA interpretation.

Given the above, the purpose of this work was to identify the mechanisms of TLA in the filament core in K8 optical glass by studying its spectral dependence.

To this end, we took advantage of TTLM, a technique capable of probing TLA dynamics at time delays of up to 300 ps with a temporal resolution of 0.45 ps and spatial resolution down to 2 μm at three probe wavelengths. This allowed us to differentiate between the plasma and TES mechanisms of light absorption and to pinpoint the possible relation between them.

## 2. Experimental

Figure 1 schematically illustrates our experimental arrangement. The pump source used was a femtosecond system involving a regenerative amplifier (*1*), which generated pulses with an energy $W = 2.5$ mJ, duration $\tau_p = 150$ fs, peak intensity wavelength $\lambda_{max} = 780$ nm and repetition rate of 1 kHz. To vary the time delay between pump and probe pulses, $\tau_{del}$, in the range 0 – 300 ps, the radiation reflected by a semi-transparent mirror (*2*) was sent to a delay line (*3*). Next, the beam was focused by a lens with $f = 15$ cm (*4*) onto a rotating sapphire disc (*5*) to produce a white-light continuum in the range 400 – 700 nm [9]. The initial continuum pulse duration almost coincided with the pump pulse duration, but the refractive index dispersion in the optical components led to pulse broadening with time.

To evaluate the probe pulse duration, we performed FTOP measurements [9]. FTOP enables imaging of a travelling light pulse in crossed polarisers owing to the pulse-induced transient Kerr-effect refractive index anisotropy. The image length in the propagation direction is determined by the cross-correlation function of the pump (150 fs) and probe pulses and can thus be used to evaluate the probe pulse duration ($\sim 300$ fs) and the temporal resolution of the entire system ($\sim 450$ fs) with allowance for the pump pulse duration. Besides, because of the

**I.V. Blonskyi, V.N. Kadan, I.A. Pavlov, N.N. Kryuchkov** Institute of Physics, National Academy of Sciences of Ukraine, prosp. Nauki 46, 03039 Kiev, Ukraine; e-mail: vikkadan@yahoo.com;
**O.I. Shpotyuk** Karat Scientific and Production Enterprise, Stryiska ul. 202, 79031 L'vov, Ukraine

Received 20 January 2009; revision received 30 June 2009
*Kvantovaya Elektronika* **39** (10) 933 – 937 (2009)
Translated by O.M. Tsarev

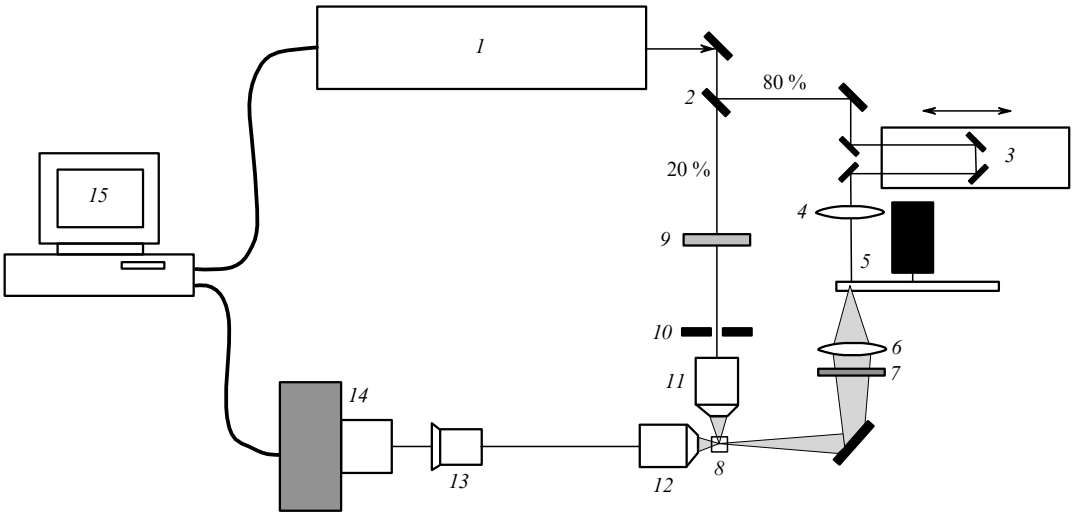


**Figure 1.** Schematic diagram of the experimental arrangement: (*1*) Legend F-1K-HE regenerative amplifier; (*2*) semi-transparent mirror; (*3*) delay line; (*4*, *6*) lenses; (*5*) medium for white-light continuum generation; (*7*) optical filter; (*8*) sample; (*9*) neutral filter; (*10*) aperture, (*11*, *12*) microscope objectives ($10^{\times}$; numerical aperture, 0.25); (*13*) eyepiece ($15^{\times}$); (*14*) CCD camera; (*15*) computer-based control system.

refractive index dispersion in the optical elements used, the longer wavelength components of the probe pulse arrive at the measurement region before the shorter wavelength components, which causes the FTOP colour image to longitudinally separate into red (R), green (G) and blue (B) parts. From the separation between the colour components, the time interval between them can be estimated as 300 fs.

The white-light probe beam was collimated by a lens with $f = 15$ cm (*6*) and focused into a $3 \times 3 \times 20$ mm sample (*8*) of K8 optical borosilicate glass (band gap of 4 eV [16]). The beam transmitted through mirror *2* was attenuated by an optical filter (*9*) and, after a circular aperture (*10*), focused by a microscope objective (*11*) into the sample (*8*) at $\sim 2.0$-mm depth, 0.5 mm from its exit face. The recording system included a microscope objective (*12*), eyepiece (*13*) and colour CCD camera (*14*). The regenerative amplifier, delay line and CCD camera were controlled by a computer (*15*).

At the pump pulse energy used, 7.5 μJ, no irreversible sample degradation was detected during the first 5–10 min, so the sample was not translated during measurements. This allowed us to considerably reduce the noise component in images by normalising them (dividing by a reference image and multiplying by the average intensity of the reference image) and to improve the accuracy in our TLA measurements in comparison with the single-pulse regime.

## 3. Results and discussion

Consider the experimental data obtained. Figure 2 shows micrographs illustrating the TLA process in K8 glass for $0 \leqslant \tau_{del} \leqslant 1.2$ ps in the G spectral region. Similar micrographs were obtained in the R and B regions. The pump beam direction in Fig. 2 is from left to right. The zero delay line position corresponded to TLA development in the field of view of the camera, without formation of a single filament. Note that this zero point is somewhat arbitrary, determined to within the accuracy in the temporal resolution of the setup. However, according to previous work, the time delay between the maximum in TLA in the filament core and the pump pulse peak is rather short: $\sim 200$ fs in K8 [9] and $\sim 50$ fs in fused silica [14]. For subsequent analysis, much longer $\tau_{del}$ times, far exceeding the uncertainty in the delay zero point, are of interest.

At an aperture diameter of 2 mm, an apertured pulse energy of 7.5 μJ and $\tau_{del} = 0$, we observed TLA onset (Fig. 2) in the form of two tracks 3 μm in diameter, which converged at the focal point with increasing $\tau_{del}$ and merged to form a single filament. On the whole, the TLA process was studied in a wide $\tau_{del}$ range (0–300 ps) with a minimal increment $\tau_{del} = 0.2$ ps. Micrographs obtained in the three spectral regions were used to evaluate the magnitude of TLA as a function of $\tau_{del}$.

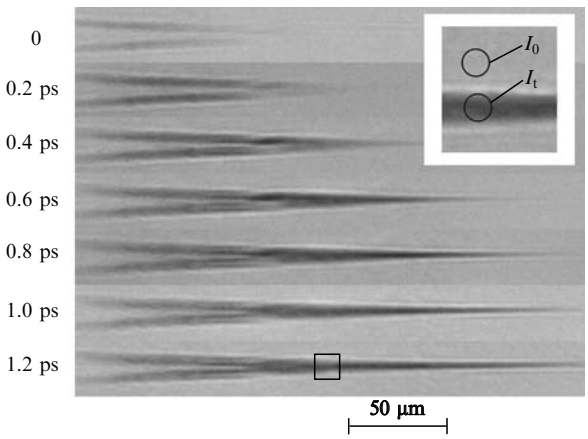


**Figure 2.** Micrographs illustrating TLA in K8 glass in the green spectral region at different time delays. The pump beam direction is from left to right.

Note that the mechanism behind the formation of TLA tracks converging to a single filament is not yet fully understood. Such tracks may be due to pump beam diffraction from aperture *10*, which produces an axial dip in the intensity distribution. Such a distribution may be due to a conical axisymmetric hollow plasma channel, which is consistent with the observed TLA pattern [19]. On

the other hand, recent work (see e.g. Ref. [9]) has shown that, when the beam power considerably exceeds a critical level, the pump beam breaks up into multiple filaments before the focal point. The observed TLA pattern can then be accounted for by the formation of two separate filaments, which subsequently merge to form a a single filament. In this paper, most attention will be paid to the mechanisms of nonequilibrium plasma relaxation in the core of an already existing filament, and the above issue will not be addressed in detail.

It is worth considering in brief the procedure for TLA ($\alpha d$, the product of the absorption coefficient and the absorbing zone length) measurements from micrographs (Fig. 2, inset). We measured the grey level intensity in the circled region of the filament, corresponding to the intensity of the transmitted probe beam, $I_t$, attenuated by the TLA process. Similarly, the grey level intensity corresponding to the initial probe beam intensity, $I_0$, was measured in the immediate vicinity of the filament (also circled in Fig. 2). The $\ln(I_0/I_t)$ value is then the absorbance, $\alpha d$. The measurement point (square at $\tau_{del} = 1.2$ ps in Fig. 2) was the same at all the $\tau_{del}$ values. It was chosen because the cross-sectional filament size at that point considerably exceeded the probe beam wavelength, which reduced the influence of probe beam diffraction by inhomogeneities on measurement results.

Figure 3 presents the $\alpha d(\tau_{del})$ data thus obtained for short (0–2 ps) and long (0–300 ps) time delays in the R, G and B spectral regions. Consider first Fig. 3a. Here, $\alpha d$ rises from zero to an almost constant level, dependent on the spectral range ($\sim 1.5$ in B and $\sim 0.15$ in R). The TLA rise time coincides with the temporal resolution of the setup. The difference between the time delays corresponding to the onset of the rise in TLA in the R, G and B regions is also of instrumental origin. As pointed out above, the R component of the probe pulse arrives at the filamentation zone before the B component and, hence, sees earlier stages of the process. It also follows from Fig. 3a that the TLA cannot be due to the formation of long-lived absorbing centres because there is no constant contribution to the absorption.

Analysis of the long-term TLA kinetics (Fig. 3b) indicates that the TLA decays in two steps. At $\tau_{del}$ shorter than $\sim 100$ ps, $\alpha d$ as a function of $\tau_{del}$ decays exponentially, with decay times $\tau_1 = 15.2 \pm 2.3$ (R), $20.0 \pm 3.0$ (G) and $24.2 \pm 7.5$ ps (B). The three confidence intervals overlap in the range $\tau_1 = 17 - 17.5$ ps. After the decay, $\alpha d$ relaxes to a constant level, then remains constant for $\tau_{del} \leqslant 300$ ps and becomes zero by the end of the 1 ms between the pulses. From single-pulse measurements of TLA in K8 glass over a wider $\tau_{del}$ range in a previous study [9], the second decay time, $\tau_2$, can be estimated at several nanoseconds. Note that the ratio of the $\alpha d$ values in the R, G and B regions is nearly the same at short ($\sim 0.5$ ps) $\tau_{del}$ ($0.15 : 0.3 : 1.5 = 1 : 2 : 10$) and long ($\sim 200$ ps) $\tau_{del}$ ($0.035 : 0.09 : 0.35 = 1 : 2.5 : 10$), suggesting that the physical mechanism of TLA remains unchanged over the entire $\tau_{del}$ range measured.

First, we will analyse the present results in relation to the mechanism of the TLA process in the filament formed. Based on the well-known fact of two-component plasma generation on the filament axis through multiphoton and/or tunnelling ionisation processes, we expected light absorption in the plasma according to the Drude model [20] to be the dominant mechanism. In this model, the absorption cross section $\sigma_{pl}$ ($\sigma = \alpha/N$, where $N$ is the concentration of absorbing centres) is determined by the pump beam frequency, $\omega$, and the carrier collision time in the plasma, $\tau_c$:

$$\sigma_{pl} = \frac{e^2}{\varepsilon_0 m_e^* c n_0} \frac{\tau_c}{(1 + \omega^2 \tau_c^2)}, \tag{1}$$

where $e$ is the electronic charge; $\varepsilon_0$ is the dielectric constant of free space; $m_e^*$ is the reduced electron mass; $c$ is the speed of light in vacuum; and $n_0$ is the refractive index of the undisturbed medium. The probe beam frequency is assumed to exceed the plasma frequency. Note that, according to estimates based on the plasma concentration attainable in femtosecond filaments $N$ ($5 \times 10^{19}$ [21] or $10^{20}$ cm$^{-3}$ [22]), the plasma frequency, $\omega_{pl} = (Ne^2/\varepsilon_0 m_e^*)^{1/2}$, is $0.7 \times 10^{15}$ or $0.5 \times 10^{15}$ s$^{-1}$, respectively, i.e., it is substantially lower

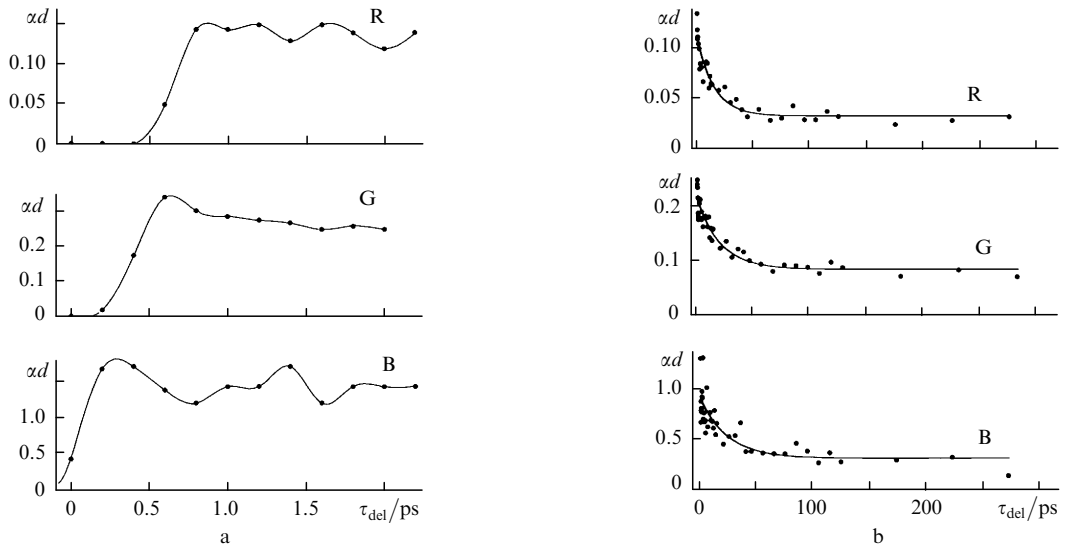


**Figure 3.** TLA dynamics in different spectral ranges. R, G and B denote the spectral ranges of the probe light corresponding to the red, green and blue transmission bands of the optical filters in the CCD array, with maxima at 640 (R), 570 (G) and 480 nm (B). $\tau_{del} = 0 - 2.2$ (a) and (b) 0–300 ps. The $\alpha d$ versus $\tau_{del}$ data are fitted with exponentials: $\tau_1 = 15.2 \pm 2.3$ (R), $20.0 \pm 3.0$ (G) and $24.2 \pm 7.5$ ps (B).

than the probe beam frequency, $\omega_R = 2.9 \times 10^{15}$ s$^{-1}$ ($\lambda_R$ = 640 nm). It follows from (1) that the absorption decreases with increasing $\omega$, whereas experimental data attest to an inverse relation, not only for steady-state $\alpha d$ values in the range 100 ps < $\tau_{del}$ < 300 ps but also for $\tau_{del} \sim 2$ ps. Therefore, at least 0.45 ps after the pump pulse (temporal resolution of the setup), it is not the plasma which makes the dominant contribution to the TLA. It is thus worth examining the contribution of TESs.

Without detailing the nature of the TESs (self-trapped excitons, trapping states, or photoinduced defects) for lack of relevant data, let us assess the effectiveness of this absorption mechanism, its time limits and its interrelation with the plasma present in the filament. To this end, we utilise the approach proposed by Martin et al. [23] for wide-gap dielectrics. TESs were represented as an ensemble of classical linear oscillators and characterised by the ground state (0) and an excited state (1) in the band gap of the dielectric. The transition between states 0 and 1 can be described by the resonance transition energy $\hbar\omega_{0-1}$, oscillator strength $f_{0-1}$ and logarithmic decrement $\gamma_{0-1}$. We neglect the contribution of the other states and assume that the hole mass considerably exceeds the electron mass. The absorption cross section $\sigma_{0-1}$ then meets the relation

$$\sigma_{0-1} = \frac{e^2 f_{0-1} \omega^2 \gamma_{0-1}}{n_0 c \varepsilon_0 m_e [(\omega_{0-1}^2 - \omega^2)^2 + \omega^2 \gamma_{0-1}^2]}, \quad (2)$$

where $m_e$ is the electron mass. Judging from the data in Fig. 3, the observed increase in $\alpha d$ with increasing $\omega$ indicates, first of all, that the present results are consistent with the TES model. Moreover, these data show that the resonance transition frequency $\omega_{0-1}$ exceeds the probe light frequency, at least in the R and G spectral regions.

Our experimental data can be used to evaluate the TES excitation energy, $\hbar\omega_{0-1}$, and the width of the corresponding transition, $\hbar\gamma_{0-1}$. To this end, we substitute the probe light frequencies at the transmission peaks of the R, G and B filters in the CCD camera into (2). Designating the respective $\sigma_{0-1}$ values as $\sigma_{01}^r$, $\sigma_{01}^g$, and $\sigma_{01}^b$, we find the $\sigma_{01}^r/\sigma_{01}^g$ and $\sigma_{01}^g/\sigma_{01}^b$ ratios and take into account that $\alpha = \sigma N_{TES}$, where $N_{TES}$ is the TES concentration. Jointly solving the two equations for $\omega_{0-1}$ and $\gamma_{0-1}$, we obtain $\hbar\omega_{0-1} = 2.7$ eV and $\hbar\gamma_{0-1} = 0.45$ eV for short $\tau_{del}$ (less than 2 ps) and $\hbar\omega_{0-1} = 2.6$ eV and $\hbar\gamma_{0-1} = 0.35$ eV for long $\tau_{del}$ (approaching 300 ps). These parameters are consistent with the conclusion drawn by Kreutz et al. [17] that the TLA in VK7 glass (an analog of K8) is due to self-trapped excitons.

It is now worth turning to TLA kinetics. Note first of all that the fact that the TES contribution to TLA prevails does not necessarily mean that all the carriers are in such states. A plasma may also be present in the sample, but the Drude absorption must be weaker than the absorption due to excitation to TESs. In particular, the presence of a plasma in soda and K9 glasses for a rather long time ($\sim$ 100 ps) after laser excitation is evidenced by recent data [18, 24], which lead us to assume that the plasma lifetime in K8 is of the same order. At the same time, as shown above the TLA in K8 is determined primarily by TESs and not by the plasma. To overcome this contradiction, we assume that $\tau_{pl} \gg \tau_{rec}$ (TES recombination time), which means that a long-lived plasma acts as a reservoir for filling TESs. The time variation of $N_{TES}$ can then be represented by the simple rate equation

$$\frac{dN_{TES}}{dt} = \frac{N_{pl}}{\tau_{tr}} - \frac{N_{TES}}{\tau_{rec}}, \quad (3)$$

where $N_{pl}$ is the plasma concentration and $\tau_{tr}$ is the time required for an electron and/or hole to be excited to such a state. The solution to Eqn (3) has the form

$$N_{TES} = N_{pl} \frac{\tau_{rec}}{\tau_{tr}} [1 - e^{(-t/\tau_{rec})}]. \quad (4)$$

Therefore, during the time characterised by the $\tau_{rec}$ constant, the TES concentration and, hence, the associated TLA will reach a steady-state level:

$$N_{TES} = N_{pl} \frac{\tau_{rec}}{\tau_{tr}}. \quad (5)$$

In our experiments, the time needed for TLA to reach a constant level was within 0.45 ps, which leads us to conclude that $\tau_{rec} < 0.45$ ps. We note in passing that $\tau_{tr} > \tau_{pl}$ because capture at TESs is not the only possible plasma recombination channel. It then follows from (5) that $N_{TES}$ is two to three orders of magnitude lower than $N_{pl}$, which is only possible when $\sigma_{0-1} \gg \sigma_{pl}$.

Finally, it is worth turning to the physics behind the fact that the TLA decay has two components, fast ($\tau_1 \sim 17$ ps) and slow ($\tau_2$ in the order of nanoseconds). As pointed out above, the finding that the ratio of the $\alpha d$ values in the R, G and B spectral regions is nearly the same over the entire range of time delays studied suggests that the nature of the TLA process remains unchanged in this range. Therefore, the rapid exponential decay of $\alpha_d$ as a function of $\tau_{del}$, with a decay time $\tau_1 \sim 17 - 17.5$ ps, may be due to an increase in $\tau_{tr}$, the time it takes for an electron and/or hole to be captured in a TES. An increase in $\tau_{tr}$ is accompanied by a reduction in $N_{TES}$ [see Eqn (5)] and, hence, in $\alpha d$. The physical interpretation of this fact is clear. Following Sun et al. [18], we attribute the rapid decay to the rapid electron relaxation to the conduction band bottom, whereas the subsequent slow (nanoseconds) decay seems to be determined by the electron lifetime in the conduction band. Initially hot carriers are more readily excited to TESs. After their thermalisation, the tunnelling mechanism prevails. For this reason, $\tau_{tr}$ has the lowest value just after the pump pulse and increases to a constant level after carrier thermalisation. For K8 glass, the carrier thermalisation time in a plasma is then $\sim$ 17 ps. Similar thermalisation times of the electron subsystem were reported for water [25] and semiconductors [26].

## 4. Conclusions

The present TTLM results indicate that the TLA relaxation in K8 glass after a filamented femtosecond pulse has two components, with decay times $\tau_1 \sim 17 - 17.5$ ps and $\tau_2 \gg 300$ ps. It follows from our results that, even though the plasma persists in the filament core for a rather long time, in excess of 300 ps, just 0.45 ps after the pump pulse the dominant contribution to the TLA comes from TESs rather than from the plasma. Analysis of the energy and rate parameters of the plasma and TESs leads us to conclude that carriers are excited to TESs from a long-lived plasma reservoir and that the TES excitation energy and the width of the corresponding transition, responsible for the TLA, are 2.6–2.7 and 0.35–0.45 eV, respectively. The first

step of the TLA relaxation, with $\tau_1 \sim 17 - 17.5$ ps, is determined by the plasma thermalisation time, whereas the second, with $\tau_2 \gg 300$ ps, is determined by the plasma lifetime.

***Acknowledgements.*** We thank the Integrated Femtosecond Laser Centre, National Academy of Sciences of Ukraine, for methodological assistance. This work was supported in part by the State Foundation for Basic Research of the Ukrainian Ministry of Education and Science (Grant No. F17/45-2007) and by the Ukrainian Science and Technology Centre (Grant No. 3745). We are indebted to I.N. Dmitruk and P.I. Korenyuk of the Integrated Femtosecond Laser Centre for their assistance with this study.

## References

1. Askar'yan G.A. *Zh. Eksp. Teor. Fiz.*, **42**, 1568 (1962).
2. Couairon A., Mysyrowicz A. *Phys. Rep.*, **441**, 47 (2007).
3. Lugovoy V.N., Prokhorov A.M. *Pis'ma Zh. Eksp. Teor. Fiz.*, **7**, 153 (1968).
4. Braun A., Korn G., Liu X., Du D., Squier J., Mourou G. *Opt. Lett.*, **20**, 73 (1995).
5. Mleinek M., Wright E.M., Moloney J.V. *Opt. Lett.,* **23**, 382 (1998).
6. Kandidov V.P., Kosareva O.G., Koltun A.A. *Kvantovaya Elektron.*, **33**, 69 (2003) [*Quantum Electron.*, **33**, 69 (2003)].
7. Kolesik M., Wright E.M., Moloney J.L. *Phys. Rev. Lett.*, **92**, 253901 (2004).
8. Kumagai H., Cho S.-H., Ishikawa K., Midorikawa K., Fujimoto M., Aoshima S., Tsuchiya Y. *J. Opt. Soc. Am. B*, **20**, 597 (2003).
9. Kadan V., Blonskyy I., Dmytruk I., Korenyuk P., Pavlov I., Puzikov V., Kryvonosov E., Lytvynov L. *Proc. SPIE–Int. Soc. Opt. Eng.*, **6726**, 67260F (2007).
10. Fujimoto M., Aoshima S., Tsuchiya Y. *Opt. Lett.*, **27**, 309 (2002).
11. Fujimoto M., Aoshima S., Hosoda M., Tsuchiya Y. *Opt. Lett.*, **24**, 850 (1999).
12. Blonskyi I., Kadan V., Shpotyuk O., Dmitruk I. *Opt. Commun.*, **282**, 1913 (2009).
13. Blonskiy I.V., Kadan V.N., Shpotyuk O.I., Dmitruk I.N., Pavlov I.A. *Pis'ma Zh. Eksp. Teor. Fiz.*, **89**, 636 (2009).
14. Blonskyi I., Kadan V., Shpotyuk O., Pavlov I. *Ukr. J. Phys. Opt.*, **10**, 100 (2009).
15. Minardi S., Gopal A., Tatarakis M., Couairon A., Tamosauskas G., Piskarskas R., Dubietis A., Di Trapani P. *Opt. Lett.*, **33**, 86 (2008).
16. Horn A., Kreutz E.W., Poprawe R. *Appl. Phys. A*, **79**, 923 (2004).
17. Kreutz E.W., Horn A., Poprawe R. *Appl. Surf. Sci.*, **248**, 66 (2005).
18. Sun Q., Jiang H., Liu Y., Wu Z., Yang H., Gong Q. *Front. Phys. China*, **1**, 67 (2006).
19. Liu W. *Appl. Phys. B*, **76**, 215 (2003).
20. Raizer Yu.P. *Zh. Eksp. Teor. Fiz.*, **48**, 1508 (1965).
21. Mao X., Mao S.S., Russo R.E. *Appl. Phys. Lett.*, **82**, 697 (2003).
22. Wu A.Q., Chowdhury I.H., Xu X. *Appl. Phys. Lett.*, **88**, 111502 (2006).
23. Martin P., Daguzan Ph., Petite G., D'Oliveira P., Meynadier P., Perdrix M. *Phys. Rev. B*, **55**, 5799 (1997).
24. Horn A., Khajehnouri H., Kreutz E.W., Poprawe P. *Proc. SPIE–Int. Soc. Opt. Eng.*, **4948**, 393 (2003).
25. Schaffer C.B., Nishimura N., Glezer E.N., Kim A.M.-T., Mazur E. *Opt. Express*, **10**, 196 (2002).
26. Huang L., Callan J.P., Glezer E.N., Mazur E. *Phys. Rev. Lett.*, **80**, 185 (1998).